

**Integrating data and theory to understand leaf-level nitrogen responses to soil nitrogen in grasslands**

Nicholas G. Smith<sup>1,\*</sup>, Elizabeth F. Waring<sup>1,2</sup>, Risa McNellis<sup>1</sup>, Evan A. Perkowski<sup>1</sup>, Jason P. Martina<sup>3</sup>, Eric W. Seabloom<sup>4</sup>, Peter A. Wilfhart<sup>4</sup>, Ning Dong<sup>5,6</sup>, Iain Colin Prentice<sup>5,6,7</sup>, Ian J. Wright<sup>6</sup>, Sally A. Power<sup>8</sup>..., Nutrient Network<sup>4</sup>

<sup>1</sup>Department of Biological Sciences, Texas Tech University, Lubbock, TX 79409, USA

<sup>2</sup>Northeastern State University

<sup>3</sup>Department of Biology, Texas State University, San Marcos, TX, 78666, USA

<sup>4</sup>Department of Ecology, Evolution, and Behavior, University of Minnesota, Saint Paul, MN 55108

<sup>5</sup>Georgina Mace Centre for the Living Planet, Imperial College London, Department of Life Sciences, Silwood Park Campus, Ascot SL5 7PY, UK

<sup>6</sup>Department of Biological Sciences, Macquarie University, North Ryde, NSW 2109, Australia

<sup>5</sup>Ministry of Education Key Laboratory for Earth System Modelling, Department of Earth System Science, Tsinghua University, Beijing 100084, China

<sup>8</sup>Hawkesbury Institute for the Environment, Western Sydney University, Sydney, Australia

\*Correspondence to:

Nicholas G. Smith

2901 Main St.

Lubbock, TX 79409

Phone: 806-834-7363

24    Email: [nick.smith@ttu.edu](mailto:nick.smith@ttu.edu)

25

## Abstract

Terrestrial carbon and nitrogen cycles are closely coupled. As such, the land surface components of Earth System Models (ESMs) are beginning to include explicit nitrogen cycles, which alter carbon cycling dynamics and, thus, climate feedbacks. An assumption embedded within these models is the positive correlation between soil nitrogen available for uptake by plants, leaf nitrogen per leaf area ( $N_{\text{area}}$ ), and photosynthetic capacity. This assumption results in greater simulated leaf assimilation capacity in systems with more available soil nitrogen. While these relationships have some empirical support, other studies have shown that  $N_{\text{area}}$  and photosynthetic capacity are primarily determined by climate and that soil nitrogen availability, instead, leads to increased development of new tissues or storage. Here, we reconcile these differences by comparing theory to data from a globally-distributed network of nutrient addition experiments in grasslands (Nutrient Network). Across the network, soil nitrogen addition increased both  $N_{\text{area}}$  and aboveground plant biomass. However, leaf traits and climate were generally better predictors of  $N_{\text{area}}$  than soil nitrogen treatment. There was a weak suggestion that the positive  $N_{\text{area}}$  response to soil nitrogen addition was strongest when plants increased allocation to leaf mass per area, but not aboveground biomass. These results reconcile discrepancies among past studies, showing that shifts in  $N_{\text{area}}$  are the function of both soil nitrogen availability and plant nitrogen demand to build biomass. It is critical to more fully understand the mechanisms underlying these dynamics for the development of the next generation of Earth System Models.

47    **Keywords**

48    Nutrient Network (NutNet), photosynthesis, water use efficiency, nutrient use efficiency, nutrient

49    allocation, C3, C4

50

## Introduction

Carbon and nitrogen cycles in terrestrial ecosystems are closely coupled (Hungate *et al.*, 2003). This coupling has a strong influence on carbon fluxes between the atmosphere and the Earth's surface (Thornton *et al.*, 2007). For instance, land plants rely on nitrogen to build photosynthetic enzymes responsible for assimilating CO<sub>2</sub> (Evans, 1989). Thus, nitrogen is an important regulator of carbon fluxes into terrestrial ecosystems, as indicated by Earth System Models (ESMs) that simulate reduced plant carbon assimilation when nitrogen constraints are imposed (Thornton *et al.*, 2007; Thomas *et al.*, 2015; Wieder *et al.*, 2015). Given ongoing addition of nitrogen to terrestrial ecosystems (Vitousek *et al.*, 1997; Galloway *et al.*, 2004, 2008), it is critical to understand how nitrogen addition will manifest itself in terrestrial ecosystems to reliably predict the rate and magnitude of future climate change.

ESMs typically assume a positive relationship between soil nitrogen availability, leaf nitrogen per unit area ( $N_{\text{area}}$ ; description of key abbreviated terms can be found in Table 1), and photosynthetic capacity (Smith & Dukes, 2013; Wieder *et al.*, 2019). The positive correlation between  $N_{\text{area}}$  and photosynthetic capacity is commonly observed (Evans, 1989; Kattge *et al.*, 2009; Walker *et al.*, 2014) and is thought to be the result of the fact that photosynthetic enzymes are typically nitrogen-rich (Evans & Seemann, 1989; Evans & Clarke, 2019). However, the positive correlation between soil nitrogen availability and  $N_{\text{area}}$  is not as straightforward. This is because plant nitrogen allocation is dynamic over time and space (Onoda *et al.*, 2017) and is a consequence of both soil nitrogen availability and tissue or organ-specific plant nitrogen demand (Paillassa *et al.*, 2020), which itself can be environmentally dependent (Perkowski *et al.*, 2021).

A few recent studies have highlighted the significantly positive relationship between soil nitrogen availability and leaf  $N_{\text{area}}$  using meta-analyses (Li *et al.*, 2020; Liang *et al.*, 2020).

74 Additionally, data from a globally distributed experiment was found to show this positive  
75 relationship as inferred from an increase in leaf nitrogen per unit leaf mass ( $N_{\text{mass}}$ ) with added  
76 soil nitrogen, but no change in leaf mass per area ( $M_{\text{area}}$ ; Firn *et al.*, 2019). These studies  
77 generally posit that this positive correlation stems from plants allocating  
78 additional nitrogen to build nitrogen-rich proteins such as Ribulose-1,5-bisphosphate (Rubisco)  
79 that are involved in carboxylation. Such reasoning generally follows previous conclusions from  
80 leaf-level analyses (Kattge *et al.*, 2009; Walker *et al.*, 2014). However, analyses on Rubisco  
81 carboxylation suggest that leaves are not commonly carboxylation-limited and are instead built  
82 to maximize the utilization of available light in a given environment at the lowest amount of  
83 Rubisco (Smith *et al.*, 2019; Peng *et al.*, 2020, 2021; Smith & Keenan, 2020). So, under nitrogen  
84 addition, an increase in leaf nitrogen to build Rubisco would be a wasteful process in the sense  
85 that the extra Rubisco would not increase photosynthesis unless it was accompanied by a similar  
86 increase in light energy. Nonetheless, a plant may allocate extra available nitrogen to build  
87 Rubisco as a means to maintain similar rates of photosynthesis at a lower stomatal conductance,  
88 effectively reducing nutrient use efficiency to increase water use efficiency (Wright *et al.*, 2003).  
89 Global studies have found empirical support for this response in some contexts (Prentice *et al.*,  
90 2014; Paillassa *et al.*, 2020).

91 Other studies have highlighted the importance of aboveground climate and light-driven  
92 nitrogen demand for predicting  $N_{\text{area}}$  (Dong *et al.*, 2017; Onoda *et al.*, 2017; Smith & Keenan,  
93 2020). Both ecophysiological theory and data (Dong *et al.*, 2017; Smith *et al.*, 2019) suggest that  
94 plant demand for nitrogen to build photosynthetic proteins decreases with temperature because  
95 enzymes work faster at higher temperature (Ali *et al.*, 2015; Dong *et al.*, 2017; Rogers *et al.*,  
96 2017; Hinojo-Hinojo *et al.*, 2018; Smith & Dukes, 2018; Smith *et al.*, 2019; Paillassa *et al.*,

2020; Smith & Keenan, 2020; Wang *et al.*, 2020) and increases with light availability to make use of additional light (Niinemets *et al.*, 2015; Dong *et al.*, 2017; Smith *et al.*, 2019; Paillassa *et al.*, 2020). In fact, previous analyses of Rubisco carboxylation capacity (Smith *et al.*, 2019; Paillassa *et al.*, 2020) and leaf nitrogen (Dong *et al.*, 2017; Firn *et al.*, 2019; Paillassa *et al.*, 2020) data suggest that climate and light-driven changes in leaf demand for nitrogen are far more important than soil nitrogen availability for predicting leaf nitrogen.

Eco-evolutionary optimality theory (Franklin *et al.*, 2020; Harrison *et al.*, 2021) provides a framework for reconciling the impact of soil nitrogen availability and plant nitrogen demand on  $N_{\text{area}}$ . Expanding upon this framework, we argue that the response of  $N_{\text{area}}$  to a change in nitrogen availability should be dependent on whole plant nitrogen demand to build new structures. Thus, an increase in nitrogen supply would increase  $N_{\text{area}}$  as a means to increase water use efficiency only when there is a limited change in biomass (Figure 1 grey dashed line). If instead plants use added nitrogen to build new structures (i.e., high stimulation of biomass), we would expect little change in  $N_{\text{area}}$  (Figure 1 black solid line). Different environmental contexts (e.g., canopy openness) may dictate variation in the biomass responses and the resulting nitrogen availability- $N_{\text{area}}$  relationship. Note that the theory, in its most holistic sense, does not differentiate between the types of structures developed (e.g., leaves, stems, roots) and could even be extended to storage or other nitrogen-dependent compounds. However, we focus here on aboveground biomass as a proxy for structural allocation to test our theory.

Here, we use leaf and biomass data from a globally distributed grassland nutrient addition experiment, Nutrient Network (NutNet; Borer *et al.*, 2014), to test these ideas about the relationship between  $N_{\text{area}}$  and structural responses to nitrogen addition. Our aims were fourfold:

- (1) Quantify and separate the impact of soil nitrogen, leaf traits, and climate on  $N_{\text{area}}$ .

(2) Assess the predictability of  $N_{\text{area}}$  from theory using aboveground climate and other leaf traits alone in comparison to belowground soil nitrogen addition.

(3) Quantify the impacts of soil nitrogen addition on aboveground biomass.

(4) Assess tradeoffs between biomass production and allocation to  $N_{\text{area}}$  under different soil nitrogen conditions.

We hypothesized that soil nitrogen addition, leaf traits, and climate would have significant separate impacts on  $N_{\text{area}}$ , but that the effect of soil nitrogen addition would be relatively weak due to the alternative ways in which plants can allocate available nitrogen (Aim 1). From this, we expected that  $N_{\text{area}}$  would be well modeled from theory based on aboveground drivers and leaf traits alone (Aim 2). We expected that soil nitrogen addition would be positively correlated with aboveground biomass on average (Aim 3). We also expected that site-level variability in this response would influence the response of  $N_{\text{area}}$  to soil nitrogen addition. Specifically, we hypothesized that the  $N_{\text{area}}$  response to soil nitrogen addition would be greatest in contexts that did not show a large increase in biomass (Aim 4).



135 **Table 1.** Description of key abbreviated terms

Variable	Units	Description
AGB	$\text{g m}^{-2}$	aboveground biomass
$\delta^{13}\text{C}$	‰	ratio of stable isotopes $^{13}\text{C}:^{12}\text{C}$
$I_g$	$\mu\text{mol m}^{-2} \text{s}^{-1}$	mean annual growing season incoming photosynthetically active radiation
$M_{\text{area}}$	$\text{g m}^{-2}$	leaf mass on an area basis
$N_{\text{area}}$	$\text{g m}^{-2}$	leaf nitrogen on an area basis
$N_{\text{mass}}$	$\text{g g}^{-1}$	leaf nitrogen on a mass basis
$N_{\text{photo}}$	$\text{g m}^{-2}$	leaf nitrogen used for photosynthesis on an area basis
$N_{\text{structure}}$	$\text{g m}^{-2}$	leaf nitrogen used for structure on an area basis
$T_g$	$^{\circ}\text{C}$	mean annual growing season temperature
$\chi$	$\text{Pa Pa}^{-1}$	ratio of intercellular to extracellular $\text{CO}_2$

136

**Figure 1.**

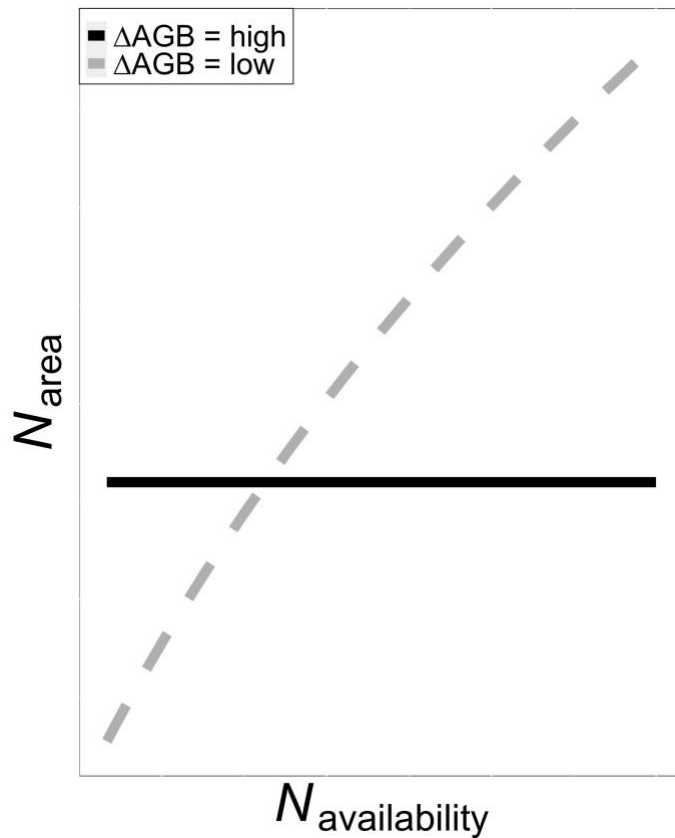


**Figure 1.** Hypothesized relationship between nitrogen (N) availability ( $N_{\text{availability}}$ ; x-axis) and leaf nitrogen per leaf area ( $N_{\text{area}}$ ; y-axis) under two different scenarios indicated by the two lines. In the first scenario (black solid line), aboveground biomass (AGB) shows a strong positive response to soil N addition. As a result, a change in  $N_{\text{availability}}$  is not reflected in changes in leaf  $N_{\text{area}}$ . In the second scenario (dashed grey line), AGB shows more muted response to soil N addition. As a result, a change in  $N_{\text{availability}}$  is reflected in a change in  $N_{\text{area}}$ . Combined, this leads to the hypothesis that the  $N_{\text{availability}}$  -  $N_{\text{area}}$  relationship should be negatively correlated with the  $N_{\text{availability}}$  - AGB relationship.

## Methods

### *Nutrient Network Description*

The Nutrient Network (NutNet; Borer *et al.*, 2014) is a network of >100 replicated nutrient addition experiments in grasslands worldwide. Each site in the network has followed a similar nutrient addition protocol, factorially adding nitrogen (N), phosphorus (P), and potassium plus a mix of macro- and micronutrients ( $K_{+μ}$ ). At each site, the experiment is set up as a randomized split-plot design with 3 replicate blocks each containing ten 5 m x 5 m plots. N, P, and K were added as urea, triple super phosphate, and potassium sulphate, respectively, at each site annually at a rate of 10 g m<sup>-2</sup> yr<sup>-1</sup>. The macro- and micronutrient mix (i.e., iron, sulfur, magnesium, manganese, copper, zinc, boron, molybdenum, and calcium) was added to all K plots once in the first year. The oldest sites in the network began adding nutrients in 2008.

### *Datasets*

To test our hypotheses, we utilized two datasets from the NutNet: (1) a leaf trait dataset (Firn *et al.*, 2019) and (2) the NutNet core dataset (Borer *et al.*, 2014). The leaf trait dataset consisted of leaf elemental, isotopic, and morphological variables. Samples were collected from up to five randomly selected individuals of different species per plot, typically 3-4 years after the start of nutrient addition at each site during peak biomass (see Firn *et al.*, 2019). For our analyses, we selected samples that contained each of nitrogen concentration ( $N_{\text{mass}}$ ; g g<sup>-1</sup>), leaf mass per area ( $M_{\text{area}}$ ; g m<sup>-2</sup>), and  $\delta^{13}\text{C}$  (‰).  $N_{\text{mass}}$  was converted to  $N_{\text{area}}$  (g m<sup>-2</sup>) using  $M_{\text{area}}$ :

$$N_{\text{area}} = N_{\text{mass}} / M_{\text{area}} \quad (1)$$

We calculated the ratio of intercellular to extracellular CO<sub>2</sub> ( $\chi$ ; Pa Pa<sup>-1</sup>) from  $\delta^{13}\text{C}$  following Farquhar *et al.* (1989) as:

$$\Delta^{13}\text{C} = (\delta^{13}\text{C}_{\text{air}} - \delta^{13}\text{C}) / (1 + \delta^{13}\text{C}) \quad (2)$$

where  $\Delta^{13}\text{C}$  (‰) is the leaf discrimination relative to air ( $\delta^{13}\text{C}_{\text{air}}$ ; ‰), assumed to be -8 ‰. For

leaves of  $\text{C}_3$  species,  $\Delta^{13}\text{C}$  was converted to  $\chi$  as:

$$\chi = (\Delta^{13}\text{C} - a) / (b_{\text{C}_3} - a) \quad (3)$$

where  $a$  and  $b$  were assumed to be 4.4‰ and 27‰, respectively (Farquhar *et al.*, 1989). For

leaves of  $\text{C}_4$  species,  $\Delta^{13}\text{C}$  was converted to  $\chi$  as:

$$\chi = (\Delta^{13}\text{C} - a) / (b_{\text{C}_4} - a) \quad (4)$$

where

$$b_{\text{C}_4} = c + d\phi \quad (5)$$

where  $c$  and  $d$  were assumed to be -5.7‰ and 30‰, respectively (Farquhar *et al.*, 1989). The

bundle sheath leakiness term ( $\phi$ ) was assumed to be 0.4. Only individuals with  $\chi$  values between

0 and 1 were used for our analyses. considered to be extreme and possibly outliers resulting from

uncertain parameters. This resulted in 2129 individuals from 208 species at 26 sites.

The NutNet leaf trait dataset was paired with the NutNet “core” dataset. This dataset consisted of data collected similarly at each NutNet site, typically on a yearly basis. From these data, we selected plot level peak biomass of living tissue measured at the same sites in the same years as the leaf trait data. Aboveground biomass (AGB; g) was sampled by hand within 0.2 m<sup>2</sup> (two 10cm x 100cm) strips in each plot and was dried before being weighed.

#### *Climate Data*

The latitude and longitude of each site were used to extract mean annual growing season temperature ( $T_g$ ; °C) and incoming photosynthetically active radiation ( $I_{g,0}$ ;  $\mu\text{mol m}^{-2} \text{s}^{-1}$ ) for each site from monthly, 1901–2015, 0.5° resolution data provided by the Climatic Research Unit

(CRU TS3.24.01) (Harris *et al.*, 2014). Growing season was operationally defined as months with mean temperatures greater than 0°C. To account for the fact that incoming photosynthetically active radiation experienced by a given plant may vary based on the density of vegetation around it, the  $I_{g,0}$  per-unit-leaf area ( $I_g$ ) was calculated as in Dong *et al.* (2017):

$$I_g = I_{g,0}(1 - e^{-kL})/L \quad (6)$$

where  $k$  is the light extinction coefficient (0.5) and  $L$  is the leaf area index, calculated from above and below canopy photosynthetically active radiation (PAR) measurements in each plot at each site:

$$L = -\log(I_{\text{below}}/I_{\text{above}})/0.86 \quad (7)$$

where  $I_{\text{above}}$  and  $I_{\text{below}}$  are above and below canopy PAR, respectively. In our analyses, we used data from 19 NutNet sites (Figure 2).

**Figure 2.**



**Figure 2.** Map of Nutrient Network sites used in this analysis (n=19).

## Analyses

To assess the drivers of  $N_{\text{area}}$  and their relative importance (Aim 1), we followed an analysis protocol similar to that described by Dong *et al.* (2017). First, we fit a linear mixed effects model with  $N_{\text{area}}$  as the dependent variable and soil treatment variables (soil N treatment, soil P treatment, soil K<sub>+μ</sub> treatment, and their respective interactions), climate ( $T_g$  and  $I_g$ ), leaf traits ( $\chi$  and  $M_{\text{area}}$ ), and species characteristics (photosynthetic pathway and whether the plant has the known capacity to biologically fix nitrogen) as fixed effects. Soil treatment and species characteristics were categorical fixed effects and climate and leaf traits were continuous fixed effects in the model. Species identity, species identity by site, and species identity by site by block were included as categorical random intercept terms.  $N_{\text{area}}$  was natural log transformed to meet normality assumptions. Predictors  $I_g$ , and  $M_{\text{area}}$  were also natural log transformed, following Dong *et al.* (2017).

We also analyzed the drivers of  $N_{\text{area}}$  from a more predictive perspective (Aim 2), again following the approach by Dong *et al.* (2017). To do this, we first calculated a prediction of the nitrogen used for photosynthesis at the leaf level ( $N_{\text{photo}}$ ) as:

$$N_{\text{photo}} = N_{\text{Rubisco}} + N_{\text{bioenergetics}} \quad (8)$$

for C<sub>3</sub> plants and

$$N_{\text{photo}} = N_{\text{Rubisco}} + N_{\text{bioenergetics}} + N_{\text{PEP}} \quad (9)$$

for C<sub>4</sub> plants. To do this, we first calculated predicted optimal rates of photosynthetic processes following Smith *et al.* (2019) as modified in Smith & Keenan (2020) for C<sub>3</sub> plants and an analogous model for C<sub>4</sub> plants by Scott & Smith (2021). Specifically, these models used measured  $\chi$  and climate variables to calculate predicted optimal maximum rates of Rubisco carboxylation ( $V_{\text{cmax},25}$ ;  $\mu\text{mol m}^{-2} \text{s}^{-1}$ ), photosynthetic electron transport ( $J_{\text{max},25}$ ;  $\mu\text{mol m}^{-2} \text{s}^{-1}$ ),

226 and phosphoenolpyruvate (PEP) carboxylation ( $V_{\text{pmax},25}$ ;  $\mu\text{mol m}^{-2} \text{s}^{-1}$ ; C<sub>4</sub> plants only), all  
 227 standardized to 25°C to better reflect an amount of enzyme in the leaf (Smith & Keenan, 2020;  
 228 Scott & Smith, 2021). Then, we calculated the predicted amount of nitrogen in Rubisco ( $N_{\text{Rubisco}}$ )  
 229 based on the model and parameterizations of Harrison *et al.* (2009):

$$N_{\text{Rubisco}} = (V_{\text{cmax},25} M_r M_n [N_r]) / (k_{\text{cat},r} n_r) \quad (10)$$

230 where  $M_r$  is the molecular mass of Rubisco, 0.55 g Rubisco ( $\mu\text{mol Rubisco}$ )<sup>-1</sup>;  $[N_r]$  is the  
 231 nitrogen concentration of Rubisco, 0.0144 mol N (g Rubisco)<sup>-1</sup>;  $M_n$  is the molecular mass of  
 232 nitrogen, 14 g N (mol N)<sup>-1</sup>;  $k_{\text{cat}}$  is the catalytic turnover at 25°C, 3,500,000  $\mu\text{mol CO}_2$  (mol  
 233 Rubisco sites \* seconds)<sup>-1</sup>; and  $n_r$  is the catalytic sites per mol Rubisco, 8 mol sites (mol  
 234 Rubisco)<sup>-1</sup>. We used  $J_{\text{max},25}$  to estimate nitrogen in bioenergetics ( $N_{\text{bioenergetics}}$ ) following the  
 235 approach by Niinemets and Tenhunen (1997):

$$N_{\text{bioenergetics}} = (J_{\text{max},25} N_{\text{cyt}}) / j_{\text{mc}} \quad (11)$$

236 where  $N_{\text{cyt}}$  is the nitrogen investment in bioenergetics (0.124 g N ( $\mu\text{mol cytochrome f}$ )<sup>-1</sup>) and  $j_{\text{mc}}$   
 237 is the activity of electron transport at 25°C (156  $\mu\text{mol electrons}$  ( $\mu\text{mol cytochrome f}$  \* seconds)<sup>-1</sup>  
 238 (Niinemets & Tenhunen, 1997).  $N_{\text{PEP}}$  was calculated in a similar manner to  $N_{\text{Rubisco}}$ , but with  
 239 PEP-specific constants:

$$N_{\text{PEP}} = (V_{\text{pmax},25} M_p M_n [N_p]) / (k_{\text{cat},p} n_p) \quad (12)$$

240 where  $M_p$  is the molecular mass of PEP, 0.41 g PEP ( $\mu\text{mol PEP}$ )<sup>-1</sup>;  $[N_p]$  is the nitrogen  
 241 concentration of PEP, assumed to be similar to Rubisco (Sage & Pearcy, 1987), 0.0144 mol N (g  
 242 PEP)<sup>-1</sup>;  $k_{\text{cat}}$  is the catalytic turnover at 25°C, 5,440,000  $\mu\text{mol CO}_2$  (mol Rubisco sites \*  
 243 seconds)<sup>-1</sup> (Boyd *et al.*, 2015); and  $n_r$  is the catalytic sites per mol PEP, assumed to be 2 mol  
 244 sites (mol PEP)<sup>-1</sup>. We also calculated the nitrogen in structural tissue ( $N_{\text{structure}}$ ) using  $M_{\text{area}}$   
 245 following the empirical approach described in Dong *et al.* (2017):

$$N_{\text{structure}} = 10^{-2.67} M_{\text{area}}^{0.99} \quad (13)$$

We then fit a second linear mixed effects model with  $N_{\text{area}}$  as the dependent variable and soil treatment variables (soil N treatment, soil P treatment, soil  $K_{+\mu}$  treatment, and their respective interactions), predicted nitrogen components ( $N_{\text{photo}}$  and  $N_{\text{structure}}$ ), and species characteristics (photosynthetic pathway and whether the plant has the known capacity to biologically fix nitrogen) as fixed effects. Soil treatment and species characteristics were categorical fixed effects and predicted nitrogen components were continuous fixed effects in the model. Species identity, species identity by site, and species identity by site by block were included as categorical random intercept terms.  $N_{\text{area}}$  was natural log transformed to meet normality assumptions.

To examine the response of community AGB to the soil treatments (Aim 3), we fit a third linear mixed effects models with AGB as the dependent variable. Soil treatment variables (soil N treatment, soil P treatment, soil  $K_{+\mu}$  treatment, and their respective interactions) were included as independent categorical variables. Site and site by block were included as categorical random intercept terms. In both cases, dependent variables were natural log transformed to meet normality assumptions.

In a final analysis, we explored the effect of soil nitrogen addition in relation to community nitrogen demand on  $N_{\text{area}}$  (Aim 4). To do this, we calculated species level  $N_{\text{area}}$ ,  $\chi$ ,  $M_{\text{area}}$ , and AGB values for all treatment types in each block at all sites. Within each treatment type within each block at each site, we calculated the percent change in  $N_{\text{area}}$  ( $\Delta N_{\text{area}}$ ; %),  $M_{\text{area}}$  ( $\Delta M_{\text{area}}$ ; %), and AGB ( $\Delta \text{AGB}$ ; %) from the ambient soil N plots to the added soil N plots. We used mean absolute deviation (Leys et al., 2013) to remove instances where any  $\Delta$  values were 3 times higher than the mean absolute deviation resulting in 328 observations. We then fit a linear mixed effects model with  $\Delta N_{\text{area}}$  as the dependent variable.  $\Delta \text{AGB}$ ,  $\Delta M_{\text{area}}$ , and their interactions



were included as independent variables. Soil treatment variables (soil P treatment, soil K<sub>+μ</sub> treatment, and their respective interactions) were also included as independent variables. Species identity, species identity by site, and species identity by site by block were included as categorical random intercept terms.

Throughout, all models were fit using the “lmer” package (Bates *et al.*, 2015) in R version 4.0.5 (R Core Team, 2019). We used Wald’s  $\chi^2$  tests to test the statistical significance of each fixed effect term in the models using the “car” package (Fox & Weisberg, 2019) in R. Post hoc analyses were done using the “emmeans” package (Lenth, 2018) in R. For the first two models, relative importance of each variable was calculated as the  $R^2$  partitioned by averaging over orders (Lindeman *et al.*, 1979) using the “calc.relimp” function in the “relaimpo” package (Grömping, 2006) in R.

All data and code used for these analyses can be found at [https://github.com/SmithEcophysLab/NutNet\\_Narea](https://github.com/SmithEcophysLab/NutNet_Narea) (DOI: XXXX).

## Results

### *Drivers of $N_{area}$ and their relative importance (Aim 1)*

Leaf nitrogen on an area basis ( $N_{area}$ ) was 28.6% greater in plots receiving nitrogen compared to plots not receiving nitrogen ( $p < 0.001$ ; Table 2). There was an interaction between soil N treatment and soil P treatment ( $p = 0.002$ ; Table 2), but post-hoc Tukey’s tests confirmed that soil N addition positively impacted  $N_{area}$  in both plots that did not receive P (35.2% increase) and plots that received P (22.5% increase;  $p < 0.05$  in both cases; Figure 2). Despite the statistically significant impact of soil nitrogen treatments on  $N_{area}$ ,  $\chi$  (5.3%),  $M_{area}$  (44.4%), and climate ( $T_g = 4.9\%$ ,  $I_g = 22.8\%$ ) had substantially higher relative importance in the model than

soil treatments (<1% combined; Table 2 and Figure 3). The positive  $N_{\text{area}}-M_{\text{area}}$  correlation (Table 2) was not surprising given equation 1. The directionality of the  $\chi$  (negative),  $T_g$  (negative), and  $I_g$  (positive) slopes (Table 2) follows from theoretical expectations. Note that despite its importance in the model, the  $N_{\text{area}}-I_g$  slope was not significantly different from 0 (Table 2). Our analysis also found that species capable of symbiotic associations with nitrogen-fixing bacteria had 102.2% higher  $N_{\text{area}}$  than species without such associations ( $p < 0.001$ ; Table 2). We also found that  $C_3$  plants had 51.6% higher  $N_{\text{area}}$  than  $C_4$  plants ( $p < 0.001$ ; Table 1). Both nitrogen fixation capacity (3.3%) and photosynthesis type (3.9%) were more important predictors in our model than the soil treatments (Table 2).

**Table 2.** Regression coefficients for linear mixed effects model with  $\ln N_{\text{area}}$  as the dependent variable and soil treatment variables, climate, leaf traits, and species characteristics as fixed effects.\*

	df	Slope	<i>p</i>	Relative Importance
Soil N	1	-	< <b>0.001</b>	1.30%
Soil P	1	-	0.184	0.56%
Soil K <sub>+μ</sub>	1	-	0.141	0.59%
<i>T<sub>g</sub></i>	1	-0.022 ± 0.006	< <b>0.001</b>	4.92%
$\ln I_g$	1	0.036 ± 0.036	0.325	22.79%
$\ln M_{\text{area}}$	1	0.907 ± 0.014	< <b>0.001</b>	44.44%
$\chi$	1	-0.141 ± 0.097	0.143	5.33%
N fixer	1	-	< <b>0.001</b>	3.26%
Photosynthetic pathway (C <sub>3</sub> /C <sub>4</sub> )	1	-	< <b>0.001</b>	3.87%
Soil N x Soil P	1	-	<b>0.002</b>	0.30%
Soil N x Soil K <sub>+μ</sub>	1	-	0.382	0.38%
Soil P x Soil K <sub>+μ</sub>	1	-	0.980	0.23%
Soil N x Soil P x Soil K <sub>+μ</sub>	1	-	0.997	0.18%

\*P-values < 0.05 are bolded and < 0.1 are italicized. Sample size is 1,561. Key:  $\chi$  = ratio of intercellular to extracellular CO<sub>2</sub> concentration,  $I_g$  = photosynthetically active radiation,  $M_{\text{area}}$  = leaf mass per leaf area,  $T_g$  = temperature. Slopes are only included for continuous fixed effects.

**Figure 2.**

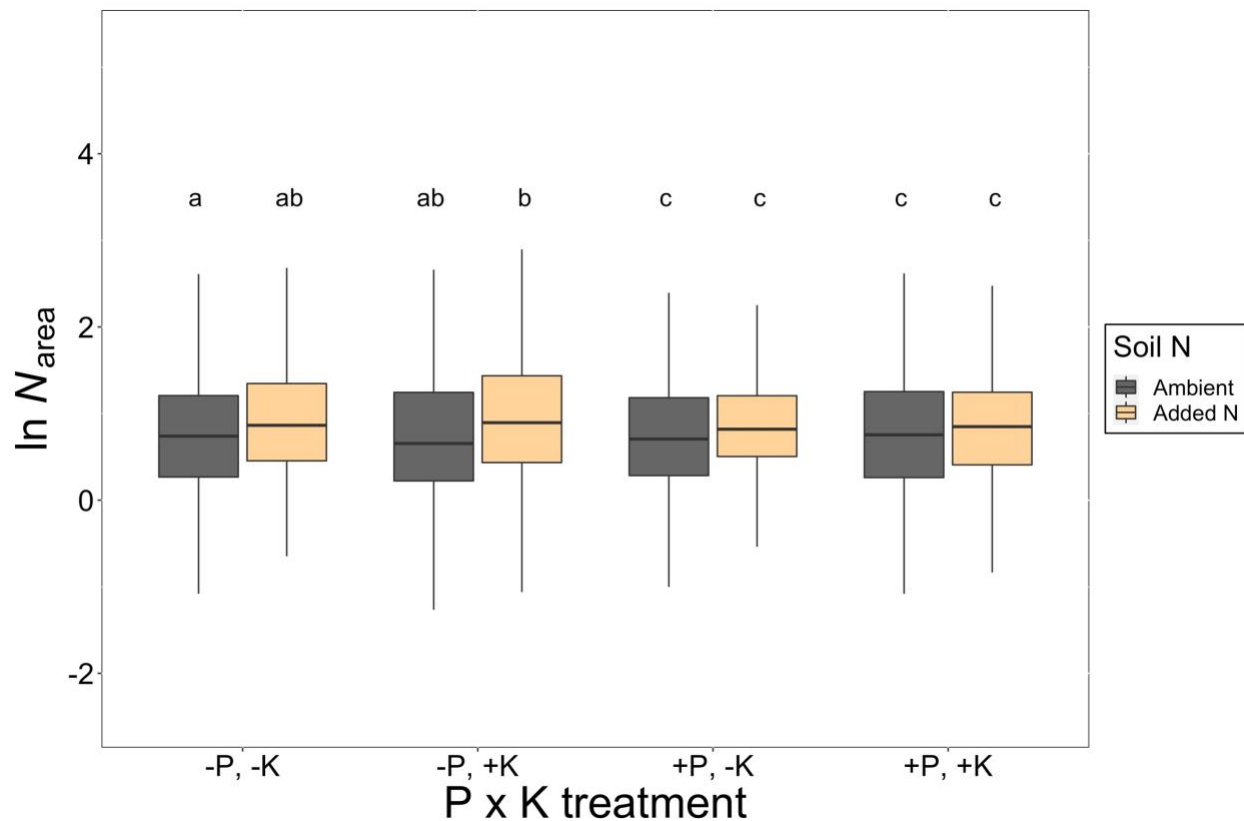


**Figure 2.**  $N_{\text{area}}$  under ambient soil nitrogen (N) and added soil N treatments in each soil

phosphorus (ambient = -P, added = +P) and soil potassium (ambient = -K, added = +K)

treatment. Boxes indicate median, first quartile, and third quartile of the observed data. Whiskers

are the furthest data point, no further than 1.5 times the inner quartile range. Lettering above

each box indicates groupings based on post-hoc Tukey's tests, where different letters indicate

statistically different groups at  $\alpha = 0.05$  across all groups shown.

**Figure 3.**

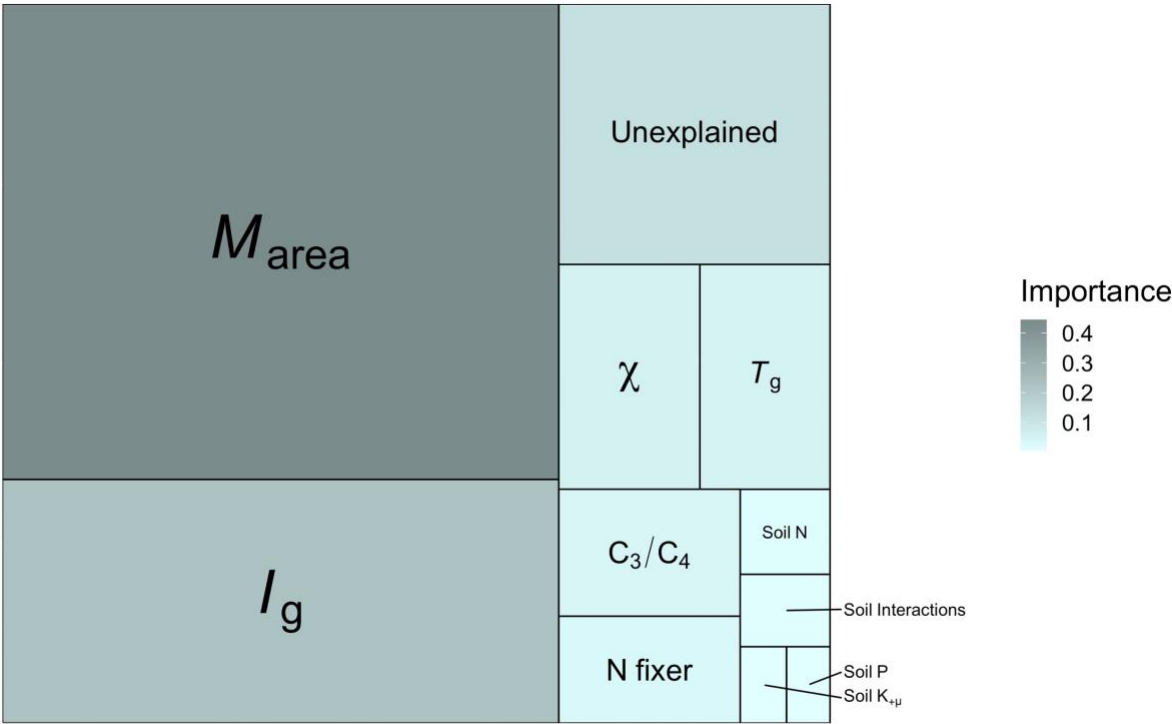


**Figure 3.** Treemap of relative importance for linear mixed effects model with  $N_{area}$  as the dependent variable and soil treatment variables, climate, leaf traits, and species characteristics as fixed effects. The area of the tree map represents 100% of the variance in the  $N_{area}$  data. The size and hue of each box is proportional to the relative importance of each factor with larger and darker boxes indicating greater importance (Table 2).

*Impacts of nitrogen demand and nitrogen availability on  $N_{area}$*

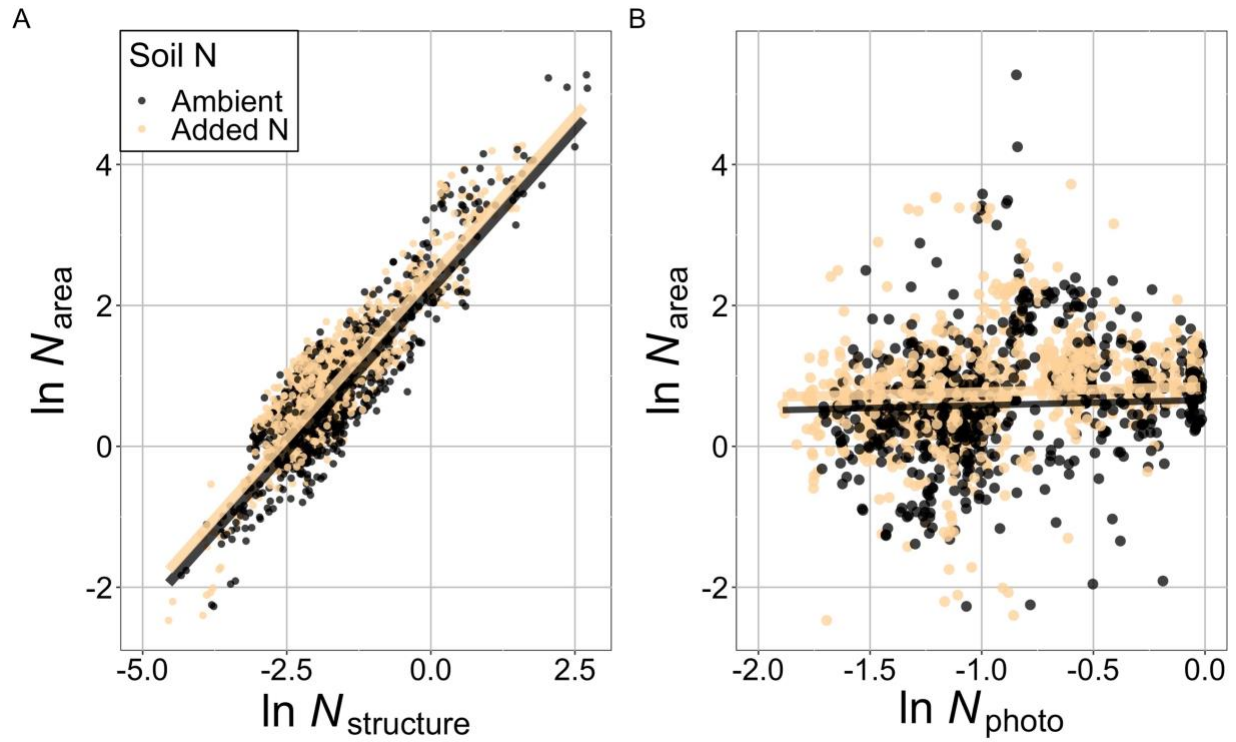
The predicted leaf N components,  $N_{photo}$  and  $N_{structure}$ , had significant, positive effects on  $N_{area}$  (Table 3 and Figure 4) and relative importance values in the model of 10.9% and 8.9%, respectively (Table 3 and Figure 5). The  $N_{photo}$  effect reflects the aboveground climate impact on  $N_{area}$ , while the  $N_{structure}$  effects reflects the impact of  $M_{area}$ . As in the first model, soil N ( $p < 0.001$ ), N fixation ( $p < 0.001$ ), photosynthetic pathway ( $p < 0.001$ ), and the interaction between soil N and soil P ( $p = 0.004$ ; Table 3) had significant effects on  $N_{area}$ . All of these trends were similar to those seen in the first model. The combined relative importance of the soil treatments was 30.1% (Table 3 and Figure 5). The relative importance of photosynthetic pathway and N fixation were 1.5% and 4%, respectively (Table 3 and Figure 5).

**Table 3.** Regression coefficients for linear mixed effects model with  $N_{\text{area}}$  as the dependent variable and soil treatment variables, predicted nitrogen components, and species characteristics as fixed effects.\*

	df	Slope	<i>p</i>	Relative Importance
$\ln N_{\text{photo}}$	1	$0.075 \pm 0.033$	<b>0.021</b>	10.91%
$\ln N_{\text{structure}}$	1	$0.914 \pm 0.014$	<b>&lt; 0.001</b>	8.89%
Soil N	1	-	<b>&lt; 0.001</b>	9.66%
Soil P	1	-	0.158	6.48%
Soil $K_{+\mu}$	1	-	0.150	6.21%
N fixer	1	-	<b>&lt; 0.001</b>	4.00%
Photosynthetic pathway ( $C_3/C_4$ )	1	-	<b>&lt; 0.001</b>	1.51%
Soil N x Soil P	1	-	<b>0.004</b>	2.60%
Soil N x Soil $K_{+\mu}$	1	-	0.383	2.53%
Soil P x Soil $K_{+\mu}$	1	-	0.949	2.14%
Soil N x Soil P x Soil $K_{+\mu}$	1	-	0.845	1.25%

\* P-values < 0.05 are bolded and < 0.1 are italicized. Sample size is 1,548. Key:  $N_{\text{photo}}$  = leaf N used for photosynthesis,  $N_{\text{structure}}$  = leaf N in structural tissue.

348 **Figure 4.**



349

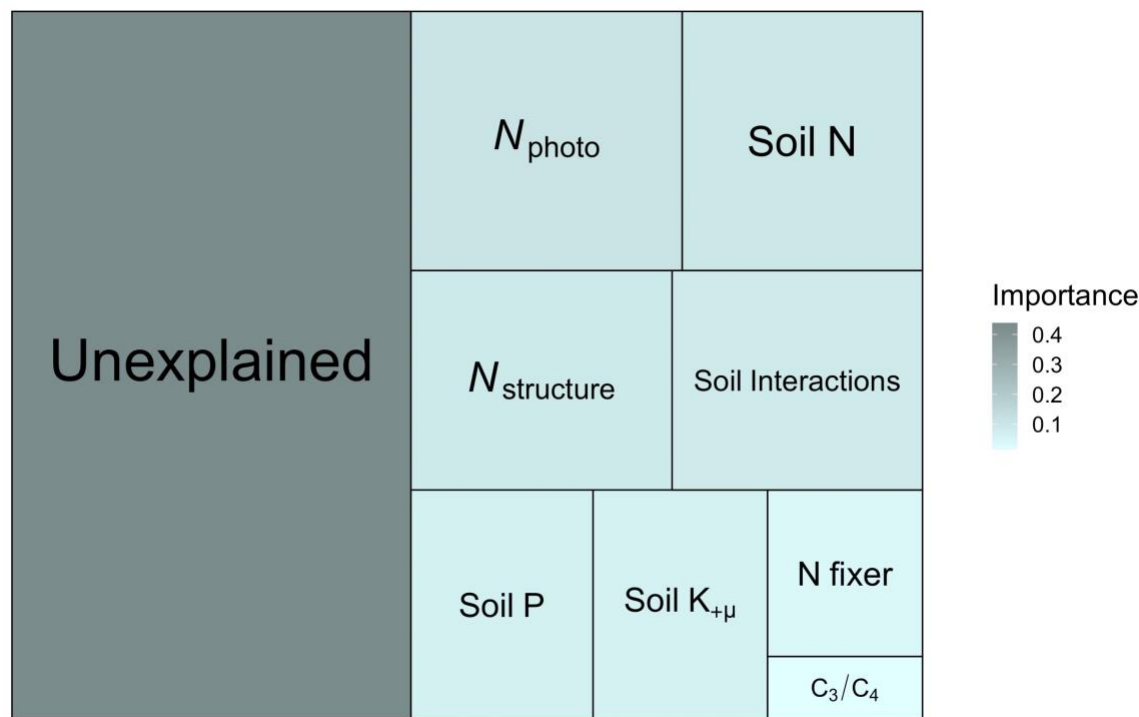
350 **Figure 4.** (A) Relationship between  $N_{\text{area}}$  and  $N_{\text{structure}}$  ( $p < 0.001$ ; Table 3) under ambient (tan)  
 351 and added (black) soil N treatments.  $N_{\text{structure}}$  and  $N_{\text{area}}$  were directly estimated from  $M_{\text{area}}$ , so the  
 352 tight correlation is not surprising. (B) Relationship between  $N_{\text{area}}$  and  $N_{\text{photo}}$  ( $p = 0.021$ ; Table 3)  
 353 under ambient and added soil N treatments. Dots represent individuals. Lines represent the  
 354 relationship predicted by the linear mixed effects model.

355

356



357 **Figure 5.**



358 **Figure 5.** Treemap of relative importance for linear mixed effects model with  $N_{area}$  as the  
359 dependent variable and soil treatment variables, predicted leaf nitrogen components, and species  
360 characteristics as fixed effects. The area of the tree map represents 100% of the variance in the  
361  $N_{area}$  data. The size and hue of each box is proportional to the relative importance of each factor  
362 with larger and darker boxes indicating greater importance (Table 3).

366 *Response of aboveground biomass to the soil treatments*

367       AGB was positively impacted by soil N (+4.4%) and P (+4.2%) amendment treatments  
368 separately (soil N:  $p < 0.001$ , soil P:  $p < 0.001$ ; Table 4 and Figure 6). There was no effect of the  
369  $K_{+μ}$  treatments or any interaction between treatments ( $p > 0.1$  in all cases; Table 4).

370

371

**Table 4.** Results for linear mixed effects model with aboveground biomass (AGB; g) as the dependent variable and soil treatment variables as independent categorical variables.\*

	<b>df</b>	<b><math>\chi^2</math></b>	<b><i>p</i></b>
Soil N	1	41.272	<b>&lt; 0.001</b>
Soil P	1	38.144	<b>&lt; 0.001</b>
Soil K <sub>+μ</sub>	1	0.735	0.391
Soil N x Soil P	1	0.026	0.871
Soil N x Soil K	1	2.243	0.114
Soil P x Soil K	1	0.074	0.786
Soil N x Soil P x Soil K	1	0.002	0.966

\* P-values < 0.05 are bolded. Sample size is 554. Key: df = degrees of freedom.

**Figure 6.**

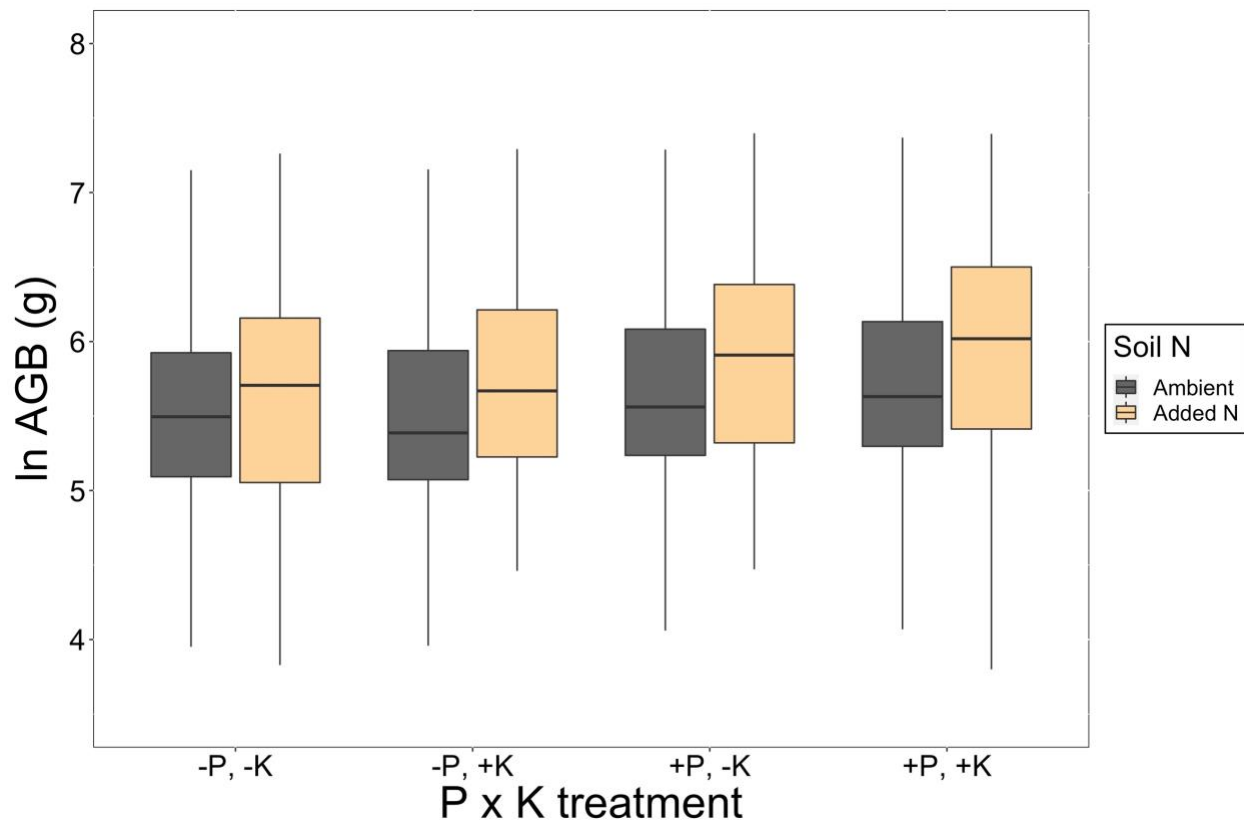


**Figure 6.** Aboveground biomass (AGB) under ambient soil N (black boxes) and added soil N (tan boxes) in each soil P x soil K<sub>+μ</sub> treatment combination (x-axis). Boxes indicate median, first quartile, and third quartile of the observed data. Whiskers are the furthest data point, no further than 1.5 times the inner quartile range.

*Effect of soil nitrogen addition in relation to community nitrogen demand on  $N_{area}$*

There was no significant effect of the response of aboveground biomass to added soil N ( $\Delta AGB$ ; %) on the response of  $N_{area}$  to added soil N ( $\Delta N_{area}$ ; %) ( $p = 0.337$ ; Table 5). However, the overall trend was negative and the slope of the interaction term between  $\Delta AGB$  and the response of  $M_{area}$  to added soil N ( $\Delta M_{area}$ ; %) suggested that the  $\Delta AGB$ - $\Delta N_{area}$  trend became more negative as  $\Delta M_{area}$  increased. We used post-hoc tests to investigate this effect. We found that the  $\Delta AGB$ - $\Delta N_{area}$  slope was indistinguishable from 0 at low  $\Delta M_{area}$  ( $\Delta M_{area} = -25\%$ ), but became slightly negative ( $p < 0.1$ ) at high  $\Delta M_{area}$  ( $\Delta M_{area} = 25\%$ ; Table 6 and Figure 7).  $\Delta N_{area}$  also increased with increasing  $\Delta M_{area}$  ( $p < 0.001$ ; Table 5 and Figure 7). Together, these responses revealed that soil N addition had the greatest stimulation on  $N_{area}$  when plants increased allocation to  $M_{area}$ , but did not increase AGB (Figure 7).

$\Delta N_{area}$  was significantly impacted by soil P ( $p = 0.002$ ), where  $\Delta N_{area}$  was greater in ambient P (19.8%) than plots with added P (9.9%) plots, confirming results from the first model presented above.

**Table 5.** Anova results for the linear mixed effects model with  $\Delta N_{\text{area}}$  as the dependent variable and  $\Delta \text{AGB}$ ,  $\Delta \chi$ , and  $\Delta M_{\text{area}}$  as independent variables.\*

	<b>df</b>	$\chi^2$	<b><i>p</i></b>
$\Delta \text{AGB}$	1	0.921	0.337
Soil P	1	10.001	<b>0.002</b>
Soil $K_{+\mu}$	1	0.063	0.803
$\Delta M_{\text{area}}$	1	117.560	<b>&lt; 0.001</b>
Soil P x Soil $K_{+\mu}$	1	0.504	0.478
$\Delta \text{AGB}$ x $\Delta M_{\text{area}}$	1	2.155	0.142

\* P-values < 0.05 are bolded and < 0.1 are italicized. Sample size is 328. Key:  $\chi$  = ratio of intercellular to extracellular  $\text{CO}_2$  concentration,  $M_{\text{area}}$  = leaf mass per leaf area.

**Table 6.** Results from Tukey’s HSD test for comparisons of means and slopes of the  $\Delta N_{\text{area}}$  linear mixed effects model.\*

	<b>Slope</b>	<b>Intercept</b>	<b><i>p</i></b>
$\Delta M_{\text{area}} = -25\%$	$0.008 \pm 0.021$	$-2.84 \pm 3.05$	<b>0.704</b>
$\Delta M_{\text{area}} = 0$	$-0.018 \pm 0.015$	$20.1 \pm 2.62$	<b>0.229</b>
$\Delta M_{\text{area}} = 25\%$	$-0.043 \pm 0.025$	$43.1 \pm 3.73$	<i>0.087</i>

\* P-values < 0.05 are bolded and < 0.1 are italicized.

**Figure 7.**

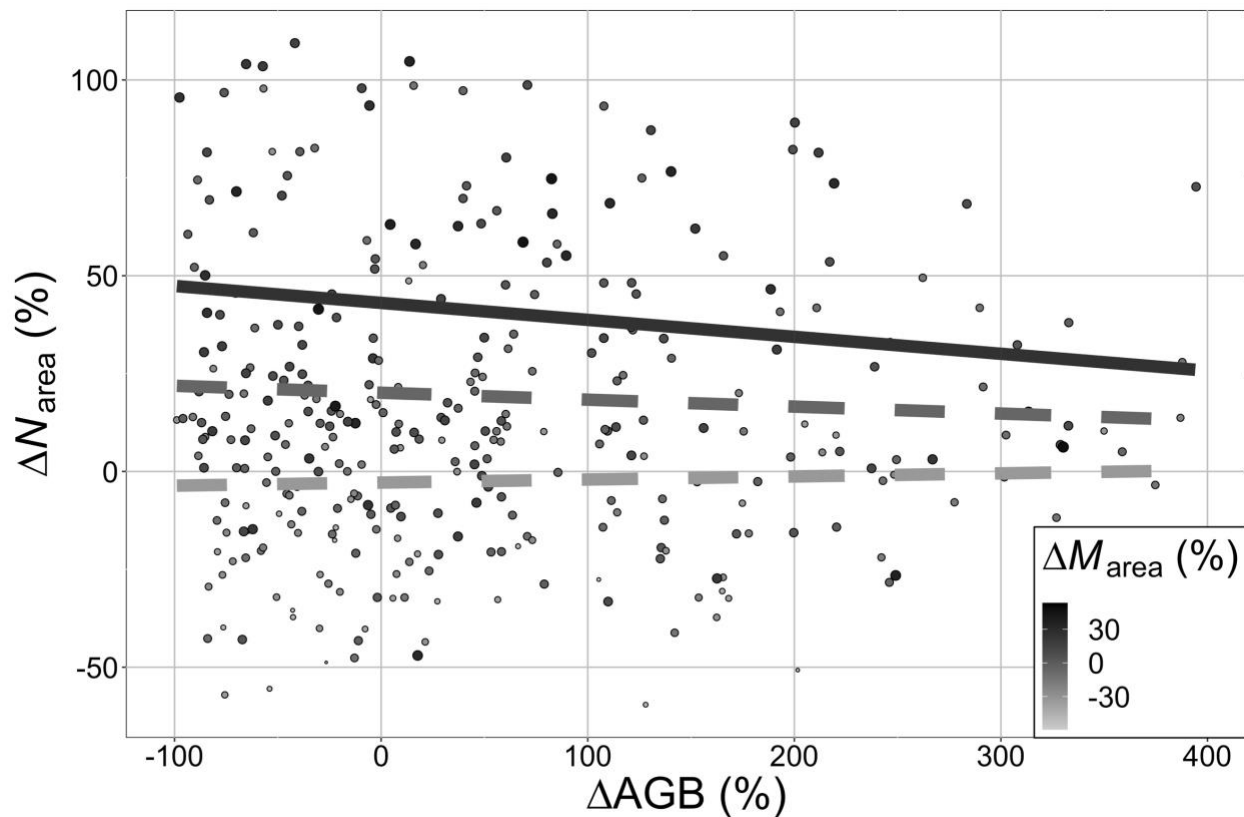


**Figure 7.** Relationship between  $\Delta N_{\text{area}}$  and  $\Delta \text{AGB}$ . Dots represent individual data points, grouped by soil P and soil  $K_{+\mu}$  treatments within a block at a site. Dots are sized and colored by  $\Delta M_{\text{area}}$ , where darker grey and larger dots indicate greater  $\Delta M_{\text{area}}$ . Lines represent the relationship predicted by the linear mixed-effects model at high ( $\Delta M_{\text{area}} = 25\%$ ;  $p = 0.087$ ; dark grey line), medium ( $\Delta M_{\text{area}} = 0\%$ ;  $p = 0.229$ ; grey line), and low ( $\Delta M_{\text{area}} = -25\%$ ;  $p = 0.704$ ; light grey line; Table 6)  $\Delta M_{\text{area}}$ . Solid lines represent a marginally significant ( $p < 0.1$ ) relationship and dashed lines represent a non-significant ( $p > 0.1$ ) relationship.



## Discussion

Accurate representation of nitrogen cycle dynamics is important for predicting terrestrial ecosystem responses and feedbacks to global change (Zaehle *et al.*, 2014; Thomas *et al.*, 2015; Wieder *et al.*, 2015, 2019). A critical aspect of these dynamics is the relationship between soil nitrogen and leaf nitrogen. Previous studies have indicated that soil nitrogen availability positively impacts leaf  $N_{\text{area}}$  through increases in  $N_{\text{mass}}$  (Firn *et al.*, 2019; Liang *et al.*, 2020). However, other studies have indicated that leaf  $N_{\text{area}}$  is also highly responsive to aboveground climate and light (Reich & Oleksyn, 2004; Borer *et al.*, 2013; Dong *et al.*, 2017; Firn *et al.*, 2019). Some even suggest that leaf nitrogen can be accurately predicted from aboveground conditions and leaf traits alone (Dong *et al.*, 2017), with the suggestion that changes in soil nitrogen availability are instead reflected in changes in biomass, as has been well-documented (LeBauer & Treseder, 2008; Fay *et al.*, 2015; Harpole *et al.*, 2017; Li *et al.*, 2020). Here, we use data from a globally-distributed grassland nutrient addition experiment to help reconcile these differences. Our results show that (1) on average, leaf  $N_{\text{area}}$  was stimulated by soil nitrogen addition, but that aboveground climate and light were stronger predictors of leaf nitrogen than soil nitrogen addition. We also show some support for the fact that (2) the impact of soil nitrogen addition on leaf  $N_{\text{area}}$  is dependent on the biomass and leaf mass per area ( $M_{\text{area}}$ ) response, with a stronger leaf nitrogen-soil nitrogen relationship when plants respond to soil nitrogen addition by allocating to  $M_{\text{area}}$ , but not biomass. Below we expand upon and contextualize these results.

### *Climate is a stronger predictor of $N_{\text{area}}$ than soil nitrogen availability*

In accordance with previous results using the same grassland nutrient addition dataset (Firn *et al.*, 2019) as well as a second study using different data (Liang *et al.*, 2020), we found

that soil nitrogen addition had a positive impact on leaf  $N_{\text{area}}$  on average across our sites. Based on the findings by Firn *et al.* (2019) using the same data, this response was primarily the result of an increase in leaf nitrogen concentration (i.e.,  $\text{g g}^{-1}$ ) in leaves when nitrogen was added to soils. This is because Firn *et al.* (2019) found that soil nitrogen addition increased  $N_{\text{mass}}$ , but had no impact on  $M_{\text{area}}$ .

Despite a significant impact of soil nitrogen addition on leaf nitrogen, our results indicate that climate and leaf traits are much stronger indicators of leaf  $N_{\text{area}}$ . We addressed this question using multiple approaches adapted from Dong *et al.* (2017). In the first approach, we assessed the relative importance of different soil, leaf trait, plant trait, and climate predictors of  $N_{\text{area}}$  in a single model. The results showed that, while statistically significant, the soil nutrient treatments were far less important than leaf traits, plant traits, and climate. Of all variables,  $M_{\text{area}}$  was the strongest predictor of  $N_{\text{area}}$  with a relative importance value of 44%. This is unsurprising given its inclusion in the  $N_{\text{area}}$  calculation (equation 1). The carbon isotope-derived ratio of intercellular to atmospheric  $\text{CO}_2$  ( $\chi$ ) was also an important predictor of  $N_{\text{area}}$  (relative importance = 5%). The negative relationship between  $N_{\text{area}}$  and  $\chi$  confirms theoretical expectations that plants maintain high  $N_{\text{area}}$  when stomata are closed (i.e., low  $\chi$ ) to maximize light utilization for photosynthesis (Wright *et al.*, 2003), a response that has been shown in observational studies (Prentice *et al.*, 2014).

Our model results also indicated that plant traits, specifically the capacity to form symbioses with nitrogen-fixing bacteria as well photosynthetic pathway, were important predictors of  $N_{\text{area}}$  with a combined relative importance value of 7%. Nitrogen-fixing plants have been previously shown to have greater  $N_{\text{area}}$  (Dong *et al.*, 2017). This may be the result of lower carbon costs to acquire nitrogen in these species (Terrer *et al.*, 2018), which might lead to greater

leaf nitrogen allocation to photosynthetic or non-photosynthetic processes (Adams *et al.*, 2016). However, nitrogen addition can also reduce the nitrogen-fixing capacity of nitrogen-fixing species (Gibson & Harper, 1985; Fujikake *et al.*, 2003; Perkowski *et al.*, 2021), which may alter the relative importance of nitrogen-fixing capability and soil nitrogen on  $N_{\text{area}}$  due to a shift in species nitrogen acquisition strategy from nitrogen fixation to direct uptake. Leaf  $N_{\text{area}}$  was also greater in  $C_4$  species than  $C_3$  species, reflecting greater nutrient costs to construct  $C_4$  leaves, confirming previous studies (Sage & Pearcy, 1987; Yuan *et al.*, 2007).

The two climate factors included in our  $N_{\text{area}}$  model (temperature and light availability) had a combined relative importance of 28%. Leaf  $N_{\text{area}}$  was negatively related to temperature, as expected from photosynthetic theory suggesting that plants optimally downregulate photosynthetic enzymes in response to increased temperature. This is because the increased enzymatic speed at higher temperatures reduces the amount of enzymes needed to maximize light utilization (Wang *et al.*, 2017). This response has been shown in the evaluation of observational temperature gradient (Smith *et al.*, 2019; Wang *et al.*, 2020) and temperature manipulation (Smith & Keenan, 2020) studies. Light availability also had high relative importance and our model indicated a positive trend, as expected based on the positive relationship between light and plant investment in photosynthetic proteins (Boardman, 1977; Niinemets *et al.*, 2015). However, the slope of this relationship was not significantly different from zero, in contrast with results from Dong *et al.* (2017).

Our second approach also supported the importance of non-soil variables for predicting  $N_{\text{area}}$ . We calculated predicted nitrogen in photosynthesis ( $N_{\text{photo}}$ ) from  $\chi$  and site climate (Smith *et al.*, 2019; Smith & Keenan, 2020; Scott & Smith, 2021). Because  $\chi$  reflects changes in climate (Prentice *et al.*, 2014; Wang *et al.*, 2017),  $N_{\text{photo}}$  served as an integrative metric for expected  $N_{\text{area}}$

responses to climate. In accordance with a similar previous study (Dong *et al.*, 2017),  $N_{\text{photo}}$  was positively correlated with  $N_{\text{area}}$  and an important predictor in our model (relative importance = 11%).  $N_{\text{photo}}$ , along with structural nitrogen calculated from  $M_{\text{area}}$ , accounted for 20% of the variability in measured  $N_{\text{area}}$ . However, an additional 31% could be accounted for from the soil nutrient treatments. This supports previous observational studies showing that soil nutrient status is an important factor to consider when predicting leaf traits (Maire *et al.*, 2015; Firn *et al.*, 2019; Smith *et al.*, 2019; Paillassa *et al.*, 2020).

#### *The impact of relative allocation to leaves and biomass on the $N_{\text{area}}$ response to soil nitrogen*

We found a positive stimulation of biomass under nitrogen addition, again supporting previous results from the same distributed experiment (Fay *et al.*, 2015; Harpole *et al.*, 2017), as well as meta-analyses of nutrient addition experiments (LeBauer & Treseder, 2008; Li *et al.*, 2020). This, combined with the significant stimulation of  $N_{\text{area}}$  by soil nitrogen addition indicated that, on average, plants at our sites were using added soil nitrogen to both increase tissue quantity (i.e., biomass) and quality (i.e.,  $N_{\text{area}}$ ). Alone, these results do not reconcile the discrepancies between previous studies.

To resolve conflicting reports about the relationship between soil nitrogen availability and  $N_{\text{area}}$  (e.g., Dong *et al.*, 2017; Firn *et al.*, 2019), we hypothesized that the strength of the relationship would be dictated by the degree to which plants use a change in soil nitrogen to build new biomass (i.e., the biomass limitation of soil nitrogen; Figure 1). Our results showed marginal support for a negative correlation between the change in biomass in response to a change in soil nitrogen and the  $N_{\text{area}}$  response to soil nitrogen availability when there was a co-occurring increase in  $M_{\text{area}}$ . This indicates that the positive soil N- $N_{\text{area}}$  relationship occurs most

strongly when soil N availability has a small impact on biomass and plants are allocating resources to leaves (indexed by a change in  $M_{\text{area}}$ ). This shows that allocation decisions are important to consider when predicting this relationship (Ghimire *et al.*, 2017).

### *Limitations*

There were unavoidable limitations to our analyses that should be considered when evaluating our results. First, we necessarily included soil nutrient availability as categorical in our analyses as we did not have data on levels of nutrient availability, only whether nutrients had been added or not. Our analyses would have been more robust had we been able to use numerical information on nutrient availability. This is because background nutrient availability was likely highly variable from site to site. Future cross-site nutrient addition studies should prioritize obtaining this information. Second, we had to necessarily rely on large scale average climate data for each site. As leaf nitrogen allocation is a dynamic process, more acute climate data may have provided more insight into the drivers of  $N_{\text{area}}$ . Finally, we lacked information on the major pools of nitrogen in leaves. Future studies that directly measure structural, photosynthetic, and other (e.g., defense) nitrogen pools would be invaluable for understanding variations in  $N_{\text{area}}$ .

### *Conclusions*

Predicting plant allocation processes across environmental gradients is difficult (Franklin *et al.*, 2012). Our results show that leaf allocation to photosynthesis and leaf mass per area can account for much of the variability in  $N_{\text{area}}$ . Importantly, theoretical approaches have shown that these traits can be reliably predicted from aboveground climate alone (Prentice *et al.*, 2014; Dong *et al.*, 2017; Wang *et al.*, 2017, 2020, 2021; Smith *et al.*, 2019; Smith & Keenan, 2020).

However, a smaller, but non-negligible amount of  $N_{\text{area}}$  variability was found to be the result of soil nitrogen. Previous studies have indicated that this can reflect variation in leaf economics, with plants choosing to shift traits towards high N use as a means to save water when N availability increases (Wright *et al.*, 2003; Maire *et al.*, 2015; Onoda *et al.*, 2017; Paillassa *et al.*, 2020). However, our results show that the biomass response to changing soil nitrogen plays a role.

Disentangling when and where plants make different allocation decisions will be critical to understand future coupled carbon-nitrogen dynamics in terrestrial ecosystems. Current ESM schemes that utilize dynamic allocation (Zhu *et al.*, 2019) or even optimization approaches (Franklin *et al.*, 2020) are good first steps for reliably predicting future responses. However, more data to test the governing assumptions in these models across space and time are needed for model evaluation and parameterization. Our study shows that this includes coupled whole-plant and leaf trait data.

## Acknowledgements

This work was generated using data from the Nutrient Network (<http://www.nutnet.org>) experiment, funded at the site-scale by individual researchers. Coordination and data management have been supported by funding to E. Borer and E. Seabloom from the National Science Foundation Research Coordination Network (NSF-DEB-1042132) and Long Term Ecological Research (NSF-DEB-1234162 and NSF-DEB-1831944 to Cedar Creek LTER) programs, and the Institute on the Environment (DG-0001-13). We also thank the Minnesota Supercomputer Institute for hosting project data and the Institute on the Environment for hosting Network meetings. NGS acknowledges funding support from the NSF (DEB-2045968), Eric and

Wendy Schmidt and Schmidt Futures, and Texas Tech University. ICP's contribution has received funding from the European Research Council (ERC) under the European Union's Horizon 2020 research and innovation programme (grant agreement No: 787203 REALM).

#### **Data and code availability**

All data and code used for these analyses can be found at [https://github.com/SmithEcophysLab/NutNet\\_Narea](https://github.com/SmithEcophysLab/NutNet_Narea) (DOI: XXXX).

#### **References**

- Adams MA, Turnbull TL, Sprent JI, Buchmann N (2016) Legumes are different: Leaf nitrogen, photosynthesis, and water use efficiency. *Proceedings of the National Academy of Sciences*, **113**, 4098 LP – 4103.
- Ali AA, Xu C, Rogers A et al. (2015) Global-scale environmental control of plant photosynthetic capacity. *Ecological Applications*, **25**, 2349–2365.
- Bates D, Maechler M, Bolker B, Walker S (2015) Fitting Linear Mixed-Effects Models Using lme4. *Journal of Statistical Software*, **67**, 1–48.
- Boardman NK (1977) Comparative photosynthesis of sun and shade plants. *Annual review of plant physiology*, **28**, 355–377.
- Borer ET, Bracken MES, Seabloom EW et al. (2013) Global biogeography of autotroph chemistry: is insolation a driving force? *Oikos*, **122**, 1121–1130.
- Borer ET, Harpole WS, Adler PB, Lind EM, Orrock JL, Seabloom EW, Smith MD (2014) Finding generality in ecology: a model for globally distributed experiments. *Methods in Ecology and Evolution*, **5**, 65–73.

582 Boyd RA, Gandin A, Cousins AB (2015) Temperature responses of C4 photosynthesis:  
 583 biochemical analysis of Rubisco, phosphoenolpyruvate carboxylase, and carbonic  
 584 anhydrase in *Setaria viridis*. *Plant Physiology*, **169**, 1850–1861.

585 Dong N, Prentice IC, Evans BJ, Caddy-Retalic S, Lowe AJ, Wright IJ (2017) Leaf nitrogen from  
 586 first principles: field evidence for adaptive variation with climate. *Biogeosciences*, **14**, 481–  
 587 495.

588 Evans JR (1989) Photosynthesis and nitrogen relationships in leaves of C<sub>3</sub> plants. *Oecologia*, **78**,  
 589 9–19.

590 Evans JR, Clarke VC (2019) The nitrogen cost of photosynthesis. *Journal of Experimental*  
 591 *Botany*, **70**, 7–15.

592 Evans JR, Seemann JR (1989) The allocation of protein nitrogen in the photosynthetic apparatus:  
 593 costs, consequences, and control. *Photosynthesis*, **8**, 183–205.

594 Farquhar GD, Ehleringer JR, Hubick KT (1989) Carbon Isotope Discrimination and  
 595 Photosynthesis. *Annual Review of Plant Physiology and Plant Molecular Biology*, **40**, 503–  
 596 537.

597 Fay PA, Prober SM, Harpole WS et al. (2015) Grassland productivity limited by multiple  
 598 nutrients. *Nature Plants*, **1**, 15080.

599 Firn J, McGree JM, Harvey E et al. (2019) Leaf nutrients, not specific leaf area, are consistent  
 600 indicators of elevated nutrient inputs. *Nature Ecology & Evolution*, **3**, 400–406.

601 Fox J, Weisberg S (2019) An R Companion to Applied Regression, Third Edition. *Sage*.

602 Franklin O, Johansson J, Dewar RC, Dieckmann U, McMurtrie RE, Brännström Å, Dybzinski R  
 603 (2012) Modeling carbon allocation in trees: a search for principles. *Tree Physiology*, **32**,  
 604 648–666.



Franklin O, Harrison SP, Dewar R et al. (2020) Organizing principles for vegetation dynamics. *Nature Plants*, **6**, 444–453.

Fujikake H, Yamazaki A, Ohtake N et al. (2003) Quick and reversible inhibition of soybean root nodule growth by nitrate involves a decrease in sucrose supply to nodules. *Journal of Experimental Botany*, **54**, 1379–1388.

Galloway JN, Dentener FJ, Capone DG et al. (2004) Nitrogen Cycles: Past, Present, and Future. *Biogeochemistry*, **70**, 153–226.

Galloway JN, Townsend AR, Erisman JW et al. (2008) Transformation of the Nitrogen Cycle: Recent Trends, Questions, and Potential Solutions. *Science*, **320**, 889–892.

Ghimire B, Riley WJ, Koven CD, Kattge J, Rogers A, Reich PB, Wright IJ (2017) A global trait-based approach to estimate leaf nitrogen functional allocation from observations. *Ecological Applications*, **27**, 1421–1434.

Gibson AH, Harper JE (1985) Nitrate Effect on Nodulation of Soybean by *Bradyrhizobium japonicum*. *Crop Science*, **25**, crops1985.0011183X002500030015x.

Grömping U (2006) Relative importance for linear regression in R: the package relaimpo. *Journal of statistical software*, **17**, 1–27.

Harpole WS, Sullivan LL, Lind EM et al. (2017) Out of the shadows: multiple nutrient limitations drive relationships among biomass, light and plant diversity. *Functional ecology*, **31**, 1839–1846.

Harris I, Jones PD, Osborn TJ, Lister DH (2014) Updated high-resolution grids of monthly climatic observations – the CRU TS3.10 Dataset. *International Journal of Climatology*, **34**, 623–642.

Harrison MT, Edwards EJ, Farquhar GD, Nicotra AB, Evans JR (2009) Nitrogen in cell walls of

628 sclerophyllous leaves accounts for little of the variation in photosynthetic nitrogen-use  
 629 efficiency. *Plant, Cell & Environment*, **32**, 259–270.

630 Harrison SP, Cramer W, Franklin O et al. (2021) Eco-evolutionary optimality as a means to  
 631 improve vegetation and land-surface models. *New Phytologist*, **23**, 2125–2141.

632 Hinojo-Hinojo C, Castellanos AE, Llano-Sotelo J, Peñuelas J, Vargas R, Romo-Leon JR (2018)  
 633 High V<sub>c</sub>max, J<sub>max</sub> and photosynthetic rates of Sonoran Desert species: Using nitrogen and  
 634 specific leaf area traits as predictors in biochemical models. *Journal of Arid Environments*,  
 635 **156**, 1–8.

636 Hungate BA, Dukes JS, Shaw MR, Luo Y, Field CB (2003) Nitrogen and Climate Change.  
 637 *Science*, **302**, 1512 LP – 1513.

638 Kattge J, Knorr W, Raddatz T, Wirth C (2009) Quantifying photosynthetic capacity and its  
 639 relationship to leaf nitrogen content for global-scale terrestrial biosphere models. *Global*  
 640 *Change Biol.*, **15**, 976.

641 LeBauer DS, Treseder KK (2008) Nitrogen limitation of net primary productivity in terrestrial  
 642 ecosystems is globally distributed. *Ecology*, **89**, 371–379.

643 Lenth R (2018) emmeans: Estimated Marginal Means, aka Least-Squares Means.

644 Li W, Zhang H, Huang G, Liu R, Wu H, Zhao C, McDowell NG (2020) Effects of nitrogen  
 645 enrichment on tree carbon allocation: A global synthesis. *Global Ecology and*  
 646 *Biogeography*, **29**, 573–589.

647 Liang X, Zhang T, Lu X et al. (2020) Global response patterns of plant photosynthesis to  
 648 nitrogen addition: A meta-analysis. *Global Change Biology*, **26**, 3585–3600.

649 Lindeman RH, Merenda P, Gold R (1979) *Introduction to bivariate and multivariate analysis*.  
 650 Scott Foresman & Co.

651 Maire V, Wright IJ, Prentice IC et al. (2015) Global effects of soil and climate on leaf  
652 photosynthetic traits and rates. *Global Ecology and Biogeography*, **24**, 706–717.

653 Niinemets Ü, Tenhunen JD (1997) A model separating leaf structural and physiological effects  
654 on carbon gain along light gradients for the shade-tolerant species *Acer saccharum*. *Plant,*  
655 *Cell & Environment*, **20**, 845–866.

656 Niinemets Ü, Keenan TF, Hallik L (2015) A worldwide analysis of within-canopy variations in  
657 leaf structural, chemical and physiological traits across plant functional types. *New*  
658 *Phytologist*, **205**, 973–993.

659 Onoda Y, Wright IJ, Evans JR et al. (2017) Physiological and structural tradeoffs underlying the  
660 leaf economics spectrum. *New Phytologist*, **241**, 1447–1463.

661 Paillassa J, Wright IJ, Prentice IC et al. (2020) When and where soil is important to modify the  
662 carbon and water economy of leaves. *New Phytologist*.

663 Peng Y, Bloomfield KJ, Prentice IC (2020) A theory of plant function helps to explain leaf-trait  
664 and productivity responses to elevation. *New Phytologist*, **226**, 1274–1284.

665 Peng Y, Bloomfield KJ, Cernusak LA, Domingues TF, Colin Prentice I (2021) Global climate  
666 and nutrient controls of photosynthetic capacity. *Communications Biology*, **4**, 462.

667 Perkowski EA, Waring EF, Smith NG (2021) Root mass carbon costs to acquire nitrogen are  
668 determined by nitrogen and light availability in two species with different nitrogen  
669 acquisition strategies. *Journal of Experimental Botany*.

670 Prentice IC, Dong N, Gleason SM, Maire V, Wright IJ (2014) Balancing the costs of carbon gain  
671 and water transport: testing a new theoretical framework for plant functional ecology.  
672 *Ecology Letters*, **17**, 82–91.

673 R Core Team (2019) R: A Language and Environment for Statistical Computing.

674 Reich PB, Oleksyn J (2004) Global patterns of plant leaf N and P in relation to temperature and  
 675 latitude. *Proceedings of the National Academy of Sciences of the United States of America*,  
 676 **101**, 11001–11006.

677 Rogers A, Serbin SP, Ely KS, Sloan VL, Wullschlegel SD (2017) Terrestrial biosphere models  
 678 underestimate photosynthetic capacity and CO<sub>2</sub> assimilation in the Arctic. *New Phytologist*,  
 679 **216**, 1090–1103.

680 Sage RF, Pearcy RW (1987) The nitrogen use efficiency of C<sub>3</sub> and C<sub>4</sub> plants: II. Leaf nitrogen  
 681 effects on the gas exchange characteristics of *Chenopodium album* (L.) and *Amaranthus*  
 682 *retroflexus* (L.). *Plant physiology*, **84**, 959–963.

683 Scott HG, Smith NG (2021) A model of C<sub>4</sub> photosynthetic acclimation based on least-cost  
 684 optimality theory suitable for Earth System Model incorporation. *Earth and Space Science*  
 685 *Open Archive ESSOAr*.

686 Smith NG, Dukes JS (2013) Plant respiration and photosynthesis in global-scale models:  
 687 incorporating acclimation to temperature and CO<sub>2</sub>. *Global Change Biology*, **19**, 45–63.

688 Smith NG, Dukes JS (2018) Drivers of leaf carbon exchange capacity across biomes at the  
 689 continental scale. *Ecology*, **99**, 1610–1620.

690 Smith NG, Keenan TF (2020) Mechanisms underlying leaf photosynthetic acclimation to  
 691 warming and elevated CO<sub>2</sub> as inferred from least-cost optimality theory. *Global Change*  
 692 *Biology*, **26**, 5202–5216.

693 Smith NG, Keenan TF, Prentice IC et al. (2019) Global photosynthetic capacity is optimized to  
 694 the environment. *Ecology Letters*, **22**, 506–517.

695 Terrer C, Vicca S, Stocker BD et al. (2018) Ecosystem responses to elevated CO<sub>2</sub> governed by  
 696 plant–soil interactions and the cost of nitrogen acquisition. *New Phytologist*, **217**, 507–522.

697 Thomas RQ, Brookshire EN, Gerber S (2015) Nitrogen limitation on land: how can it occur in  
698 Earth system models? *Global change biology*, **21**, 1777–1793.

699 Thornton PE, Lamarque J-F, Rosenbloom NA, Mahowald NM (2007) Influence of carbon-  
700 nitrogen cycle coupling on land model response to CO<sub>2</sub> fertilization and climate variability.  
701 *Global Biogeochemical Cycles*, **21**, GB4018.

702 Vitousek PM, Aber JD, Howarth RW et al. (1997) Human alteration of the global nitrogen cycle:  
703 sources and consequences. *Ecological applications*, **7**, 737–750.

704 Walker AP, Beckerman AP, Gu L et al. (2014) The relationship of leaf photosynthetic traits –  
705 V<sub>c</sub>max and J<sub>max</sub> – to leaf nitrogen, leaf phosphorus, and specific leaf area: a meta-analysis  
706 and modeling study. *Ecology and Evolution*, **4**, 3218–3235.

707 Wang H, Prentice IC, Keenan TF et al. (2017) Towards a universal model for carbon dioxide  
708 uptake by plants. *Nature Plants*, **3**, 734–741.

709 Wang H, Atkin OK, Keenan TF et al. (2020) Acclimation of leaf respiration consistent with  
710 optimal photosynthetic capacity. *Global Change Biology*, **26**, 2573–2583.

711 Wang H, Colin Prentice I, Wright IJ, Qiao S, Xu X, Kikuzawa K, Stenseth NC (2021) Leaf  
712 economics explained by optimality principles. *bioRxiv*, 2021.02.07.430028.

713 Wieder WR, Cleveland CC, Smith WK, Todd-Brown K (2015) Future productivity and carbon  
714 storage limited by terrestrial nutrient availability. *Nature Geoscience*, **8**, 441.

715 Wieder WR, Lawrence DM, Fisher RA et al. (2019) Beyond static benchmarking: Using  
716 experimental manipulations to evaluate land model assumptions. *Global Biogeochemical*  
717 *Cycles*, **33**, 2018GB006141.

718 Wright IJ, Reich PB, Westoby M (2003) Least-cost input mixtures of water and nitrogen for  
719 photosynthesis. *The American Naturalist*, **161**, 98–111.

720 Yuan Z, Liu W, Niu S, Wan S (2007) Plant Nitrogen Dynamics and Nitrogen-use Strategies  
 721 under Altered Nitrogen Seasonality and Competition. *Annals of Botany*, **100**, 821–830.  
 722 Zaehle S, Medlyn BE, De Kauwe MG et al. (2014) Evaluation of 11 terrestrial carbon–nitrogen  
 723 cycle models against observations from two temperate Free-Air CO<sub>2</sub> Enrichment studies.  
 724 *New Phytologist*, **202**, 803–822.  
 725 Zhu Q, Riley WJ, Tang J, Collier N, Hoffman FM, Yang X, Bisht G (2019) Representing  
 726 Nitrogen, Phosphorus, and Carbon Interactions in the E3SM Land Model: Development and  
 727 Global Benchmarking. *Journal of Advances in Modeling Earth Systems*, **11**, 2238–2258.  
 728